

Chapter 5

Cumulative Distribution Sharpness Profiling

'The oldest, shortest words - 'yes' and 'no' - are those which require the most thought.'

-Pythagoras

There is always some gray area between the two extremities and the degree of gray reveals some interesting characteristics. When a bearing signal is traversed temporally this degree of gray, between the fault and non-fault regions, generates a profile revealing the nature of the fault.

Highlights:

- Bearing fault signal shows inherent cyclostationarity under constant operating speed and becomes non-stationary under varying speed conditions.
- It shows a sharper distribution having narrower peak, as opposed to the flatter peaks of noise.
- A method of generating a profile of local distribution sharpness values is proposed to improve the prominence of fault curves in the time-frequency domain.
- The proposed algorithm is shown to be better than the conventional signal enveloping method for the representative cases of UOO-2018.

Bearing fault signal shows inherent cyclostationarity even under constant operating speed [182]. However, if the speed shows fluctuations, then the signal becomes non-stationary. Such speed deviations largely affect the notion of bearing fault diagnosis because the fault characteristic frequencies (FCF) are multiples of operational speed. As the FCFs vary with speed, it is impossible to diagnose bearing faults using envelope spectrum alone. Thus the non-stationarity needs to be taken into consideration before diagnosing the faults.

Extraction of instantaneous frequency from the TFR is a well-explored topic. Earlier research on extracting instantaneous frequency (IF) from the TFR includes Wigner-Ville distribution with an adaptive window length [183]. But, bearing signatures are multicomponent signals and the diagnosis needs the information about the operational speed as well as the bearing fault characteristic frequencies. Extraction of instantaneous frequencies from the TFR using image processing algorithms is proposed in [184]. This method often shows unexpected jumps in the extracted curve. To overcome this problem the ridge curve extraction using fast path optimization is introduced in [185] and applied to bearing fault diagnosis in [152, 153]. This method extracts multiple curves from the TFR (MTFCE). One of these curves is identified as the operational speed and the mean of ratios between other curves and the operational speed are used for fault diagnosis. Unlike the order tracking based methods, this method only uses the information from the TFR to diagnose the faults. This method is a benchmark for the data made available in [168] and correctly classifies the fault in most of the cases, however, it fails in many cases. The authors have given two important reasons for this failure, contamination of the signal by random noise and interference and inability to extract the operational speed from the TFR. They have also proposed a modification of this method to overcome the disadvantages [186].

The proposed approach is fundamentally different than the available methods. Instead of calculating the envelope of the bearing signal, it is proposed to calculate its cumulative distribution sharpness (CDS) profile, which is further analysed using short-time Fourier transform and MTFCE. In this chapter, it is first shown that CDS is a potential candidate for locally separating the fault and non-fault regions in the vibration signal as it follows

monotonicity and continuity, which are essential characteristics of any classifier [187]. Using an example of inner race fault case under constant speed condition, the methodology is then explained. Then for several cases of UOO-2018 dataset, the results are discussed. The proposed method is shown to have an added advantage that the CDS profiling gives a smooth envelope-like resultant signal. Thus there is no need to calculate the envelope of the raw vibration signal. Additionally, it is also shown to generate TFR with more prominent fault curves.

5.1 Theoretical Background

In this subsection, the *Laplace* and *Normal-Laplace (NL)* distributions are first discussed, followed by the evidences showing that bearing fault signals follow these distributions. The effect of noise on cumulative distribution sharpness (CDS) is also investigated.

5.1.1 Laplace Distribution

Bearing signatures show sharper and narrower peaks compared to Gaussian distributed noise. A study on probability distribution of bearing fault signatures shows its Laplace nature [188, 189].

If a bearing signature (y) is contaminated by additive white Gaussian noise (ε), then the fault signal (x) is given by -

$$x(t) = y(t) + \varepsilon(t) \quad (5.1)$$

Assuming (y) follows the Laplace distribution, its probability distribution function (PDF) is given by -

$$f(y) = \frac{1}{\sqrt{2}\sigma_l} \exp\left(-\frac{\sqrt{2}|y-\mu|}{\sigma_l}\right) \quad (5.2)$$

Three representative bearing fault signals are considered - (a) mathematical model as given in [190], (b) experimental data from Case Western Reserve University (CWRU)

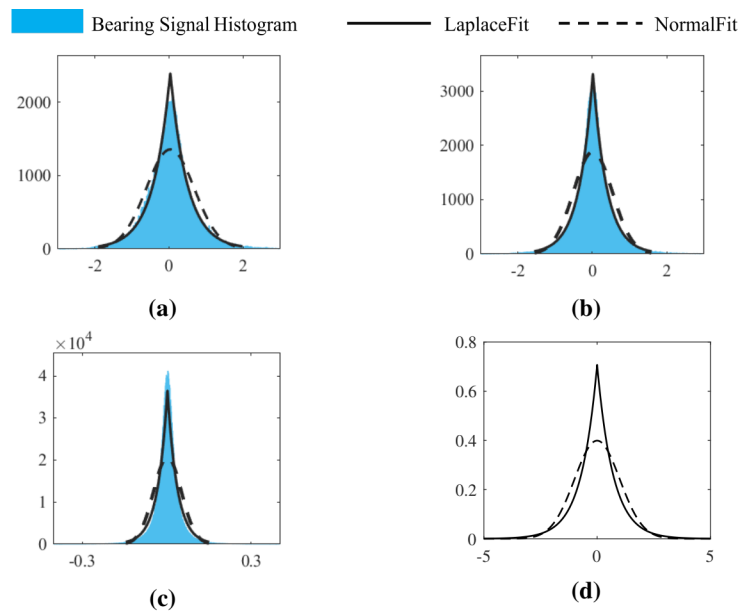


Figure 5.1: Distribution fitting (a) mathematical model as given in [190], (b) experimental data in [167] and (c) experimental data in [168] (d) Laplace and normal distribution of equal variance.

under constant operational speed [167] and (c) experimental data under variable operating speed given in [168]. The findings are shown in Fig. 5.1 (a,b,c).

Fig. 5.1 (d) shows representative PDFs of Laplace and normal distributions of equal variance, plotted using their mathematical functions. It can be observed that the bearing signatures follow Laplace distribution.

5.1.2 Normal-Laplace (NL) Distribution

Laplace distribution has a sharper peak at the mean value compared to the Normal distribution. But, when contaminated with noise, the peak flattens. For additive white Gaussian noise, the resultant PDF becomes the convolution of Laplace and normal distribution PDFs (*NL* distribution) [191, 192]. Thus for zero mean, symmetric *NL* distribution the PDF is calculated as -

$$\begin{aligned}
f(x) = & \frac{\sigma_l}{4\sqrt{2}} \left[\exp\left(\frac{\sigma_l}{2\sqrt{2}}\left(-2x + \frac{\sigma_l\sigma_g^2}{\sqrt{2}}\right)\right) \operatorname{erfc}\left(\frac{\sigma_g}{2} - \frac{x}{\sqrt{2}\sigma_g}\right) \right. \\
& \left. + \exp\left(\frac{\sigma_l}{2\sqrt{2}}\left(2x + \frac{\sigma_l\sigma_g^2}{\sqrt{2}}\right)\right) \operatorname{erfc}\left(\frac{\sigma_g}{2} + \frac{x}{\sqrt{2}\sigma_g}\right) \right] \quad (5.3)
\end{aligned}$$

The cumulative distribution function (CDF) of *NL* distribution can be calculated by integrating above equation as-

$$\begin{aligned}
F(x) = & \frac{1}{4} \left[2 - \exp\left(\frac{1}{\sqrt{2}\sigma_l}\left(-2x + 2\sigma_g^2\right)\right) + \operatorname{erf}\left(\frac{x}{\sqrt{2}\sigma_l}\right) \right. \\
& + \exp\left(\frac{1}{\sqrt{2}\sigma_l}\left(-2x + \frac{\sqrt{2}\sigma_g^2}{\sigma_l}\right)\right) \operatorname{erfc}\left(\frac{-\sigma_g}{\sigma_l} + \frac{x}{\sqrt{2}\sigma_l}\right) \\
& \left. + \exp\left(\frac{1}{\sqrt{2}\sigma_l}\left(2x + \frac{\sqrt{2}\sigma_g^2}{\sigma_l}\right)\right) \operatorname{erfc}\left(\frac{\sigma_g}{\sigma_l} + \frac{x}{\sqrt{2}\sigma_l}\right) \right] \quad (5.4)
\end{aligned}$$

-where σ_g and σ_l are the standard deviations of the normal and Laplace distributions respectively. $\operatorname{erf}(\cdot)$ and $\operatorname{erfc}(\cdot)$ are the error function and complementary error function respectively.

The cumulative distribution sharpness (CDS) is defined in terms of its slope as the ratio of percentage rise from 10% to 90% of $F(x)$ to percentage run from $x|_{F(x)=10\%}$ to $x|_{F(x)=90\%}$. To show that the CDS is a valid and potential candidate to quantify the noise contamination in bearing fault signals, it is tested on important properties that any classifier must possess - monotonicity and continuousness [187]. The CDF in Eq. 5.4 is simulated for different values of noise variance (σ_g^2) under constant signal variance (σ_l^2).

5.1.3 Effect of Noise on CDS

The distribution sharpness is typically less in those cases of [167] in which the accelerometer is mounted away from the faulty bearing (Fig. 5.2(b)). (For example, if the faulty bearing is present at the drive end, then the accelerometer is located at the fan end). It also reduces when the noise is added to the model in [190] or data in [168] (Fig. 5.2(a,c)). The

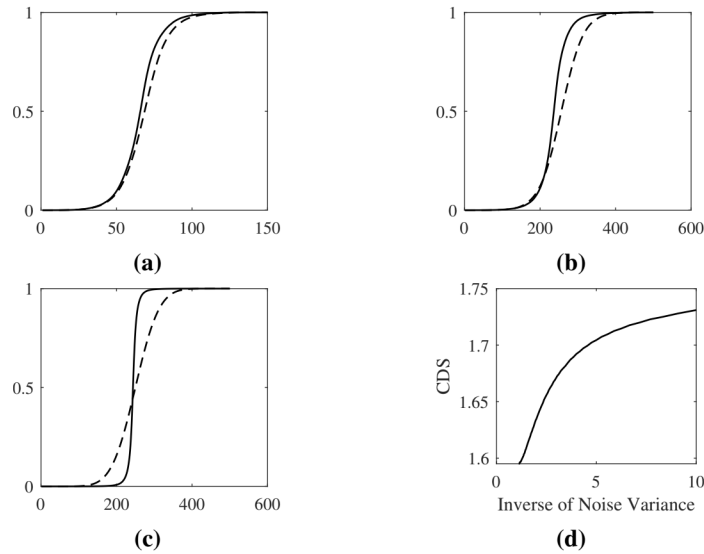


Figure 5.2: Effect of noise on distribution sharpness (a) mathematical model as given in [190] (‘—’ No noise, ‘- - -’ SNR = 10 dB), (b) experimental data in [167] (‘—’ accelerometer located near the faulty bearing, ‘- - -’ accelerometer located away from the faulty bearing), (c) experimental data in [168] (‘—’ No noise, ‘- - -’ SNR = 10 dB) (d) Non-decreasing and continuous nature of CDS.

effect of noise on the distribution sharpness can be clearly understood from Fig. 5.2(d), in which CDS is plotted against the inverse of noise variance. As the noise variance decreases, the signal-to-noise ratio (SNR) increases. Evidently, the value of CDS is found to be larger for larger SNR.

The results, as shown in Fig. 5.2 (d), confirm that the CDS monotonously increases for decreasing values of noise variance. The simulation is carried out with smaller increments ($\Delta\sigma_g^2 = 0.01$) of noise variance to check the continuity. This signifies that for a faulty bearing the presence of Gaussian noise can be quantified using CDS. Larger the CDS, smaller is the noise contamination and vice versa. This validates the use of CDS as a measure of bearing fault under the influence of noise. It is proposed to use this idea for locally quantifying the presence of noise in the windowed signal and generate a profile to be further analysed by short-time Fourier transform. In the next subsection, the details of generating such a profile are discussed, followed by an example.

5.2 Proposed Algorithm

Fig. 5.3 shows the flow-chart of cumulative distribution sharpness profiling (CDSP). It needs sampling rate (f_s), fault characteristic frequency (f_f) and signal length (N) as inputs. As the fault characteristic frequency (f_f) is a multiple of operational speed of the rotating machine, either the measured speed (f_{rps}) or its estimate is required.

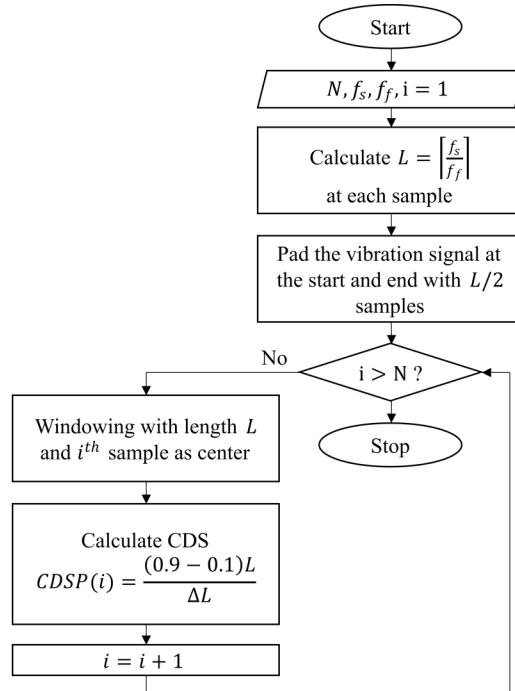


Figure 5.3: Proposed cumulative distribution sharpness profiling (CDSP) (N - Number of samples in the signal, f_s - Sampling frequency, f_f - Fault characteristic frequency, L - Window length, ΔL - Fraction of L in which CDF varies from 0.1 to 0.9, CDS - Cumulative distribution sharpness of the windowed signal, $CDSP$ - CDS profile obtained by sweeping a window over bearing vibration signal.)

To estimate sharpness of the CDF, the data from windowed signal is fitted to Laplace distribution and then the ratio of 80% rise in the CDF (from 0.1 to 0.9) to the percentage of window length in which this change occurs, is calculated. This choice of points to estimate the slope is due to the sigmoidal shape of the cumulative distribution function. As the 'S' shaped sigmoidal function saturates at both ends to 0% and 100%, the rise from 10% to 90% provides a linear region to estimate the sharpness.

If $C(x) = P(X \leq x)$ is the estimated CDF fit of windowed signal, L is the window length (in number of samples) and ΔL is the number of samples in which $C(x)$ changes from 0.1 to 0.9, then we define the sharpness (CDS) as -

$$\text{CDS} = \frac{0.8L}{\Delta L} \quad (5.5)$$

The profile of CDS is obtained by sweeping a Hanning window over the vibration signal and calculating the CDS of the windowed signal. That is, if the window size is L , then the CDS is calculated for samples 1 to L after windowing, then for samples 2 to $L + 1$, for samples 3 to $L + 2$ and so on. The window length (L) is made adaptive by making it inversely proportional to the bearing characteristic frequency. This ensures that the bearing fault features are captured even under variable speed conditions. To diagnose inner race and outer race faults, this process is performed twice - once each with characteristic frequency of inner race (f_{ir}) and of outer race (f_{or}). The fault characteristic frequency can be calculated as $M \times f_{rps}$, where M is a multiplication factor that depends on fault location and bearing geometry. Thus, for inner race fault diagnosis (IR), the window length is chosen as $L = f_s / f_{ir}$ and for outer race diagnosis (OR) as $L = f_s / f_{or}$.

To demonstrate the CDS Profiling operation an inner raceway defect from MFPT bearing fault dataset is used [193]. The raw vibration signal is acquired at a rate of 48.8 KHz under constant rotational speed of 25 Hz. The fault characteristic frequency of inner race is 118.8Hz. For this case, the CDS profile is calculated using two different window types - Hanning and Mexican hat, as shown in Fig. 5.4. Three important observations from this figure are -

- The profiles maintain the periodicity of the fault signature. The fundamental period of inner race fault frequency is around 8 ms, which can be observed in both the profiles. The profiles show local extrema, of which, maxima correlate to the fault regions and minima represent the non-fault regions.
- The profiles have envelope-like appearance, that is, the high-frequency resonance

is removed and the low-frequency fault signature is retained. Conventionally, such demodulation is achieved using Hilbert transform. Thus, CDS Profiling removes the need of Hilbert transform.

- Comparison of profiles obtained using Hanning and Mexican hat windows shows that the Hanning window performs better as the profile obtained using Hanning window is smoother compared to that of Mexican hat window.

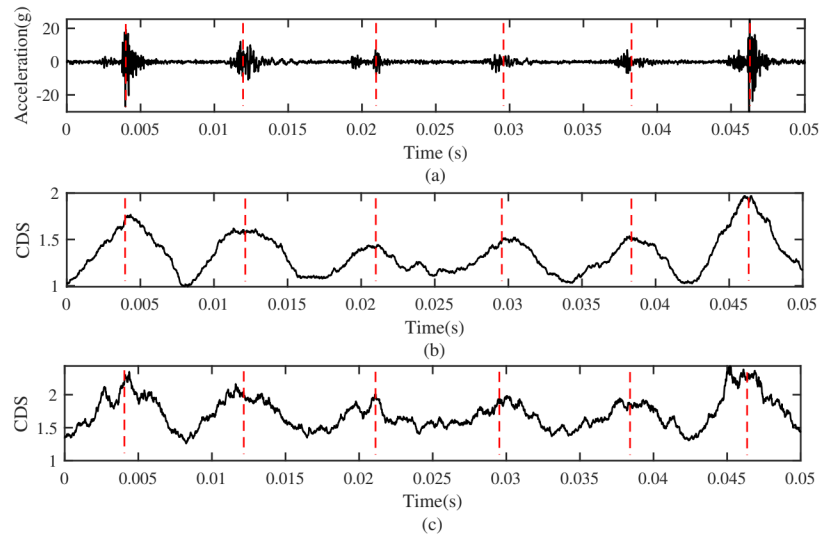


Figure 5.4: Effect of window type on CDSP. CDSP using (b) Hanning and (c) Mexican hat window

5.3 Results

The proposed method for bearing fault diagnosis under variable speed conditions is validated some representative cases of the UOO-2018 dataset. Details of this dataset can be found in Chapter 3.

5.3.1 Cumulative Distribution Sharpness Profile

First, an inner race fault case (IA2) is considered for demonstrating the importance of CDSP. Fig. 5.5 shows the raw vibration signal, the corresponding envelope signal and the

CDSP.

The important observations from Fig 5.5 are -

- Considering the inner race fault frequency (119.2 Hz), there are 4 fault regions in the vibration signal, separated by 0.0084 sec each.
- Regions *C* and *D* are easier to identify, whereas regions *A* and *B* are suppressed.
- The proposed CDSP gives local peaks corresponding to all the four regions. These local peaks in CDSP depend on the cumulative distribution of the samples in that region.
- CDSP gives a smoother profile compared to signal enveloping, thus removing the high frequency component and emphasizing on the periodicity of the fault. This is reflected in the time-frequency representation of the signal with increased prominence of the fault curve.

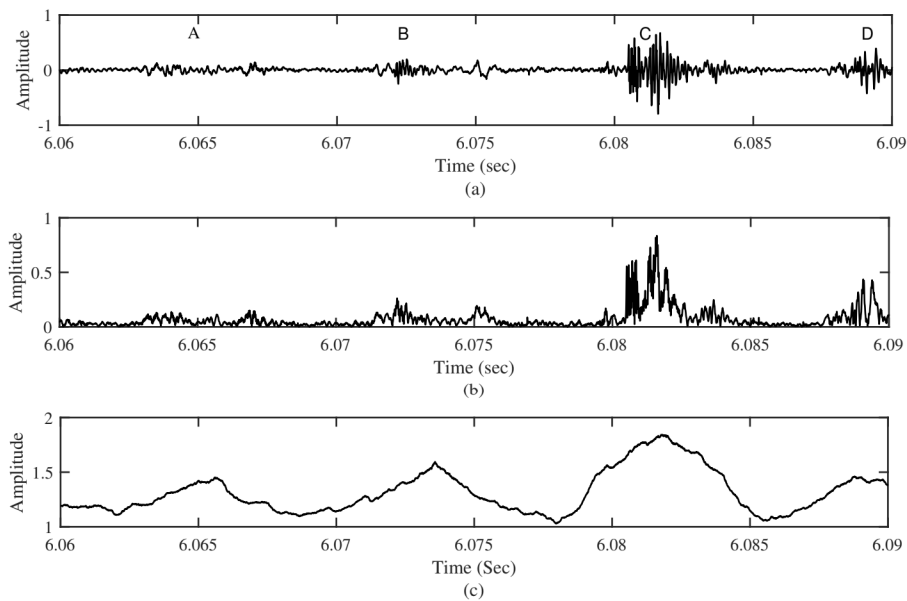


Figure 5.5: Importance of cumulative distribution sharpness profile. Case IA2 : (a) Raw vibration signal, (b) Signal envelope (Hilbert transform), (c) Cumulative Distribution Sharpness Profile

5.3.2 Inner race fault case

The *IAI* case is taken as a representative, in which the rotational speed is increasing from 12.5 to 27.8 Hz. The spectrogram, shown in Fig. 5.6(a), is obtained from inner race fault diagnosis and has clearly distinguished inner race fault frequency increasing from 68 to 151 Hz approximately. The spectrogram from the outer race diagnosis also shows the same frequency, which asserts the fact that the periodicity present in CDS Profiles is not induced by the choice of window length. Even though the outer race frequency (f_{or}) is used to calculate the window length, prominence of inner race frequency is observed in the spectrogram. But, optimum result is obtained if the inner race frequency (f_{ir}) is used. Comparatively, the inner race frequency is less prominent in the spectrogram of signal envelope.

It is also interesting to note that because of improved prominence, first curve obtained from TFR ridge curves extraction (MTFCE) is the estimated fault curve which closely follows the theoretical fault frequency. For the original signal enveloping, the estimated fault curve is often the second or third curve extracted.

5.3.3 Outer race fault case

Outer race fault is often elusive in variable speed conditions because it falls in very low frequency region. However, the outer race fault diagnosis can still be improved. A representative case *OAI*, in which the rotational speed increases from 15 to 27 Hz approximately, is considered. All three spectrograms (Fig. 5.7) show less prominent outer race fault curve. The curve obtained from outer race diagnosis of proposed method contributes more to prominence measure as compared to other two spectrograms. In the original signal envelope spectrogram, other curves are almost equally prominent.

5.3.4 Rolling Element Fault

Rolling element fault is indeed a common and most elusive type of fault in bearings. The applicability of the proposed method is investigated to rolling element faults. It is

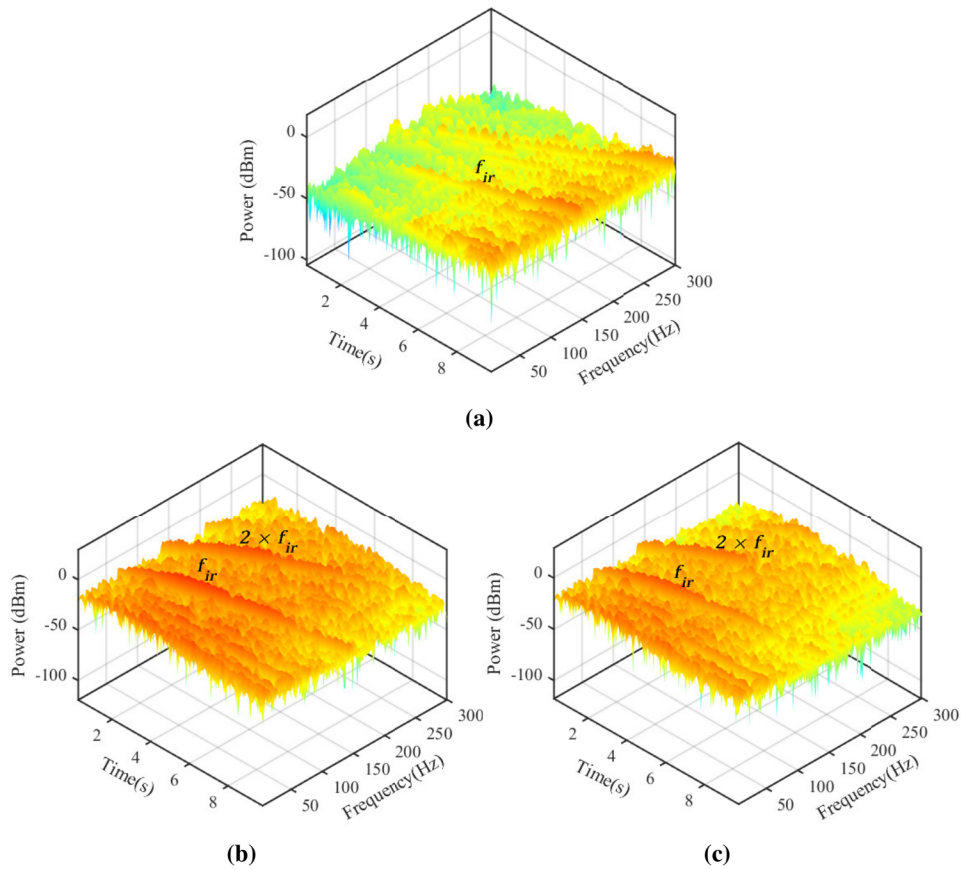


Figure 5.6: Case IA1 : Time-frequency representation using spectrogram of (a) Original signal envelope (b) CDSP with window length corresponding to f_{ir} (c) CDSP with window length corresponding to f_{or} . (f_{ir} , the fault characteristic frequency of inner race, is prominent in (b).)

observed that such faults do not follow Laplace distribution. They rather follow a normal distribution and are thus difficult to be separated from the noise. The global distribution of a representative rolling element fault case is shown below. It is evident that the proposed model is not suitable for such faults.

5.4 Conclusion

Bearing fault signal is inherently cyclostationary, but under variable speed conditions it becomes completely non-stationary. The standard fault diagnosis methods, like fast kurtogram, are insufficient in this case. One of the earliest methods to deal with such cases is order-tracking, which includes signal resampling either using dedicated hardware or

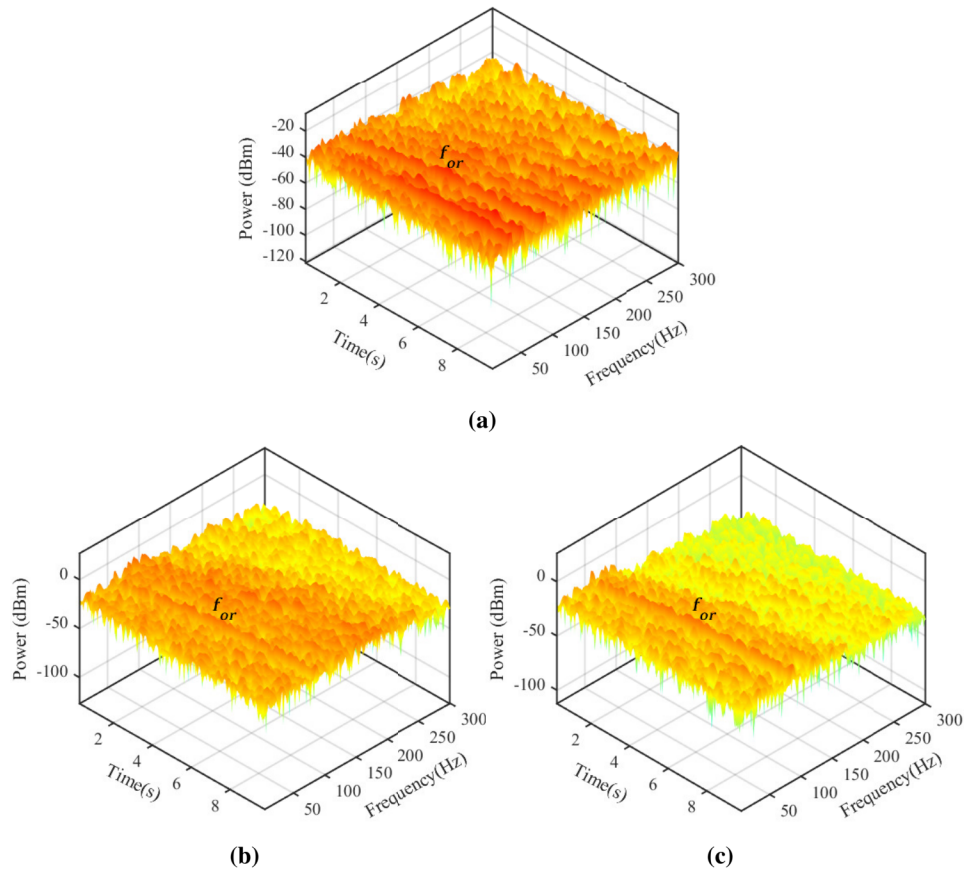


Figure 5.7: Case OA1: Time-frequency representation using spectrogram of (a) Original signal envelope (b) CDSP with window length corresponding to f_{ir} (c) CDSP with window length corresponding to f_{or} . (f_{or} , the fault characteristic frequency of outer race, is prominent (c).)

sophisticated software. Such hardware is often expensive and unreliable. On the other hand, computed order-tracking using software heavily relies on interpolation. Instantaneous frequency curves extraction from the time-frequency domain representation is an efficient method to overcome these drawbacks, but it also poses several challenges.

In this chapter, a windowing based signal processing method, named cumulative distribution sharpness profiling (CDSP), is proposed to improve the results of time-frequency ridge curve extraction. The sharpness of cumulative distribution function is first shown to be a valid measure of locally separating the fault and non-fault regions of the signal. It is shown to follow two important characteristics - monotonicity and continuousness. The theoretical Laplace distribution function with additive white Gaussian noise is simulated

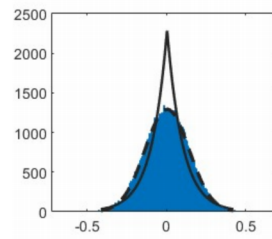


Figure 5.8: Histogram of a rolling element fault case from CWRU-2013

to validate these properties. Then, it is proposed that a profile of local CDS values be generated as a new signal. Such a profile is found to be a smooth envelope-like signal which retains the periodicity of the original signal. Through a series of examples from public dataset, it is shown that the proposed method of CDS profiling improves the prominence of the fault curve in the time-frequency domain representation. The overall diagnosis results are discussed in next chapter by comparing the results of existing signal processing methods.



This document was created with the Win2PDF "print to PDF" printer available at <http://www.win2pdf.com>

This version of Win2PDF 10 is for evaluation and non-commercial use only.

This page will not be added after purchasing Win2PDF.

<http://www.win2pdf.com/purchase/>